Applied Physics Letters

Intrinsic role of ↑↑↓↓-type magnetic structure on magnetoelectric coupling in Y_2NiMnO_6

Cite as: Appl. Phys. Lett. **116**, 242901 (2020); https://doi.org/10.1063/5.0009568
Submitted: 01 April 2020 . Accepted: 02 June 2020 . Published Online: 15 June 2020

Chao Xin, Bingqian Song, Zhixin Sun, Zhongxiang Hu, Boshi Yuan, Hui Li, Guangyong Jin, and Feng Pan

Applied Physics Letters ARTICLE scitation.org/journal/apl

Intrinsic role of ↑↑↓↓-type magnetic structure on magnetoelectric coupling in Y_2NiMnO_6

Cite as: Appl. Phys. Lett. **116**, 242901 (2020); doi: 10.1063/5.0009568
Submitted: 1 April 2020 · Accepted: 2 June 2020 ·
Published Online: 15 June 2020

Chao Xin,[1,a] Bingqian Song,[2] Zhixin Sun,[1] Zhongxiang Hu,[3] Boshi Yuan,[1] Hui Li,[1] Guangyong Jin,[1,a] and Feng Pan[3,a]

AFFILIATIONS

[1]School of Science, Changchun University of Science and Technology, Jilin Key Laboratory of Solid-State Laser Technology and Application, Changchun 130022, China
[2]Department of Physics, Harbin Institute of Technology, Harbin 150001, People's Republic of China
[3]School of Advanced Materials, Peking University Shenzhen Graduate School, Shenzhen 518055, China

[a]**Authors to whom correspondence should be addressed:** xinchao@pkusz.edu.cn, jgycust@163.com, and panfeng@pkusz.edu.cn

ABSTRACT

Structure-property correlations are a major challenge in the investigation of magnetoelectric multiferroic materials. We have systematically investigated the intrinsic role of ↑↑↓↓-type order in magnetoelectric coupling in Y_2NiMnO_6. The calculated results reveal that the ferromagnetic (FM) order is the magnetic structure of the ground state and the total energy of ↑↑↓↓-type order is close to that of the FM order. The electric polarization is calculated to be 0.78 $\mu C/cm^2$ along the crystallographic b-axis for $U_{Ni} = U_{Mn} = 3$ eV. In addition to the exchange-striction mechanism, a more noticeable contribution from redistribution of polarized charge is found in our study. Magnetic hysteresis loops show the ferromagnetism in Y_2NiMnO_6, which can be explained by magnetic field-induced spin flop transition from the E-type to FM order. Our DFT + U theoretical investigations also proposed a switching adiabatic path of magnetoelectric coupling, in which the 180° reverse of electric polarization is driven by rotation of spins.

Type-II multiferroics in which the ferroelectrics are driven by magnetic order have attracted considerable attention due to their potential application in the magnetic field control of ferroelectricity or electric field control of magnetism.[1–5] However, low Curie temperature and weak magnetoelectric coupling remain the two principal problems, limiting their application in spin electronic devices.[6,7] Therefore, it is a great challenge to search new multiferroics with excellent performance, and the current research mainly focuses on type-II magnetoelectric multiferroics.[8] In the last few decades, several type-II multiferroics have been found where electric polarization is related to either the specific type of collinear or non-collinear spin order.[9] The exchange striction mechanism is responsible for ferroelectricity in collinear spin order,[10] while the occurrence of electric polarization as a result of non-collinear spin ordering is explained by the inverse Dzyaloshinskii–Moriya interaction[11] or in some p-d orbital hybridization cases.[12] Until recently, the concept of multiferroic quantum criticality was proposed and candidate materials in which the phenomenon can take place were suggested.[13]

The exchange-striction mechanism often emerges in multiferroics with up–up–down–down (↑↑↓↓) type magnetic order, such as perovskite manganates $RMnO_3$ (R = rare earth ions) with E-type magnetic order[14] and the Ising spin chain magnet Ca_3CoMnO_6.[15] Based on the model Hamiltonian, early theoretical studies show that the magnetic state changes from a FM (R=La) to an E-type (R = Y), i.e., Y_2NiMnO_6 (YNMO) has a ground state of E-type magnetic order.[16] But recently, experimental investigations have shown that the double perovskite YNMO displays ferromagnetic order (FM), and the magnetic transition temperature is $T_c \approx 81$ K.[17] In addition, a recent study on magnetic-driven multiferroic behavior of YNMO is in contrast to the study by Zhu *et al.* There are explicit differences between their magnetic and dielectric properties.[18] The magnetic domain wall between ↑↑ and ↓↓ FM order can lead to electric polarization.[19] Moreover, from the structural and energy point of view, Zhou *et al.* have explained the origin of ferroelectric in YNMO, in which the relative displacements between Ni and Mn make the two out-of-plane Ni–O–Mn bond angles as well as the Ni–Mn distance unequal and weaken the out-of-plane Ni–Mn super-exchange interaction.[20] These experimental and theoretical results are puzzling since the net magnetization and the E-type antiferromagnetic (AFM) order are mutually exclusive, and magnetic order-induced electric polarization should disappear in FM order.

In the present work, we systematically study the magnetic order of the ground state, exchange interactions, the origin of ferroelectricity, spin flop transition, and adiabatic path of magnetoelectric by using DFT+U calculations. Combining with the existing experimental results, we reveal that the FM order is the ground state. Magnetic hysteresis loops show the ferromagnetism in YNMO, which can be explained by magnetic field-induced spin flop transition from E-type to FM order. Our DFT+U theoretical investigations also proposed a switching adiabatic path of magnetoelectric coupling, in which the 180° reverse of electric polarization is driven by rotation of spins.

All of our first-principles calculations, including geometry optimization and electronic structure, are based on spin polarized density functional theory (DFT) as implemented in the Vienna *ab initio* simulation package (VASP).[21,22] The Perdew–Burke–Ernzerhof functional revised for solids (PBEsol) was adopt for exchange-correlation potential. Generalized gradient approximation (GGA)[23] with the Hubbard parameter (GGA+U)[24] was employed to solve the Kohn–Sham equation.[25] The plane wave energy cutoff, convergence in energy, and residual force on each atom are set to 500 eV, 1×10^{-5} eV, and 0.01 eV/Å, respectively. In order to obtain the accurate ↑↑↓↓-type and E-type magnetic order, we build a $1 \times 1 \times 2$ and $2 \times 1 \times 1$ supercell, and the corresponding Brillouin zone integrations were set using a tetrahedron method in a $6 \times 6 \times 2$ and $4 \times 4 \times 4$ Monkhorst–Pack K-point mesh.[26] Spin–orbital coupling (SOC) and magnetic anisotropy were ignored. The Berry Phase method with a $10 \times 10 \times 10$ mesh was adopted to evaluate electric polarization (FE).[27] The structure and spin density visualization and analysis were carried out using the VESTA code.[28]

The crystal structure of YNMO at room temperature has the monoclinic symmetry with space group $P2_1/n$ (point group C_{2h}) (Fig. 1).[29] In order to identify the magnetic structure of ground states, we have calculated the total energy of six collinear magnetic orders: ferromagnetic (FM), A-type, C-type, G-type, E-type, and ↑↑↓↓-type antiferromagnetic.[30] The scheme diagram of six magnetic order is plotted in Fig. S1. The E-type magnetic order corresponding to the ↑↑↓↓-type antiferromagnetic along the (101)-plane, if the magnetic anisotropy is ignored, is also the same as that of ↑↑↓↓-type antiferromagnetic along the c-axis, as depicted in Fig. 1. Both E- and ↑↑↓↓-type order can break the spatial-inversion symmetry and further lower the crystal symmetry to the $P2_1$ space group (point group C_2). The energy differences between FM and other five AFM were calculated with different values of U_{eff} for Ni and Mn ions, which are listed in Table I. It is clear that the energies of the FM orders are lower than those of all AFM order, confirming the FM order to be the magnetic structure of ground states. To have a further understanding of the structural distortions caused by the magnetic configuration, we also optimize the structural parameters for all the magnetic states. As we denote in Fig. 1, the Ni–O–Mn angles corresponding to the bonds with parallel and antiparallel spins are defined as θ_p and θ_{ap}. The θ_p values for FM are larger than θ_{ap} values for other AFM order in the entire U range [see Fig. S2(a)]. However, when both θ_p and θ_{ap} are present in the ↑↑↓↓-type order, this difference is even more obvious, which explains the more obvious exchange-striction in ↑↑↓↓-type order.

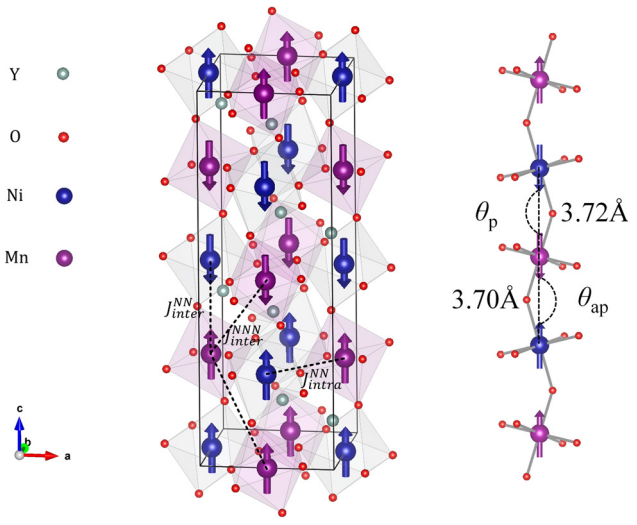

FIG. 1. Crystal structure and ↑↑↓↓-type order of YNMO. The dotted lines denote the intra-plane and inter-plane exchange paths between nearest-neighbor and next-nearest-neighbor spins. θ_p and θ_{ap} denote the Ni–O–Mn super-exchange angle with parallel and anti-parallel spin.

The exchange integral paths were extracted by mapping the total energies to the Heisenberg Hamiltonian, where J_{ij} includes all the nearest-neighbor (NN) and next-nearest-neighbor (NNN) exchange interactions as shown in Fig. 1. The intra-plane Ni–Ni/Mn–Mn exchange coupling for all magnetic order is ferromagnetic coupling, which can be attributed to E_0, and the values of J^{NNN}_{inter} exchange interactions should be the average of Mn–Mn and Ni–Ni exchange couplings. The evaluated exchange integrals were shown as functions of U_{eff} values for Ni ions with fixed U_{eff} = 3 eV for Mn ions [see Fig. S2(b)],

$$E = E_0 - \sum_{(i,j)} J_{ij} S_i \cdot S_j. \quad (1)$$

The exchange integrals of considered magnetic configurations in the $1 \times 1 \times 2$ supercell with a normalized spin quantum number can be written as

$$E_F = E_0 - 32J^{NN}_{intra}S_{Ni}S_{Mn} - 16J^{NN}_{inter}S_{Ni}S_{Mn} - 64J^{NNN}_{out}S_{Mn}S_{Mn}, \quad (2)$$

$$E_{\uparrow\uparrow\downarrow\downarrow} = E_0 - 32J^{NN}_{intra}S_{Ni}S_{Mn}, \quad (3)$$

$$E_A = E_0 - 32J^{NN}_{intra}S_{Ni}S_{Mn} + 16J^{NN}_{inter}S_{Ni}S_{Mn} + 64J^{NNN}_{inter}S_{Mn}S_{Mn}, \quad (4)$$

$$E_C = E_0 + 32J^{NN}_{intra}S_{Ni}S_{Mn} - 16J^{NN}_{inter}S_{Ni}S_{Mn} + 64J^{NNN}_{inter}S_{Mn}S_{Mn}, \quad (5)$$

TABLE I. Calculated total energies (meV) depend on different AFM orders as functions of U_{eff} values for Ni ions. The U_{eff} value for Mn is fixed to be 3 eV. The total energies of FM order were set as zero.

U	↑↑↓↓	A	C	G	E
1	66.23	170.09	393.89	565.88	299.15
2	64.18	153.99	351.48	500.14	283.25
3	61.79	141.71	318.94	450.25	264.22
4	58.16	131.35	291.84	409.11	246.44
5	55.01	121.68	268.72	372.82	230.43
6	52.52	113.43	249.42	344.10	215.70

$$E_G = E_0 + 32J_{intra}^{NN}S_{Ni}S_{Mn} + 16J_{inter}^{NN}S_{Ni}S_{Mn} - 64J_{inter}^{NNN}S_{Mn}S_{Mn}. \quad (6)$$

Since $S = 3/2$, $|S|^2 = S(S+1) = 3.25$ for Mn^{4+} and $S = 1$ and $|S|^2 = S(S+1) = 2$ for Ni^{2+}. As we can see from Fig. S2(b), the two NN exchange interactions are FM for all the U_{eff} values. The NN exchange integrals are obviously stronger than the NNN exchange integrals. Because the competition from J_{inter}^{NNN} can be ignored, the close energy between FM order and ↑↑↓↓-type order is related to J_{inter}^{NN}. In YNMO, the FM ground state can be transformed into ↑↑↓↓-type order when meeting the condition $J_{inter}^{NN} + 4J_{intra}^{NNN} < 0$ according to the above formulas: $E_{\uparrow\uparrow\downarrow\downarrow} < E_F$, while the additional energy gain caused by the exchange-striction effect in ↑↑↓↓-type order was not evaluated in the above equations. The asymmetric exchange interactions in neighbor FM and AFM spin pairs would lead to the off-central structural distortion and then divide into two different J_{out}^{NN} values. Within the mean-field approximation, we also estimate the transition temperature $T_C \sim 75$–80 K for $U_{Ni} = U_{Mn} = 3$ eV, which is very close to the measured experimental value of $T_C \sim 81$ K.[17] Thus, $U_{Ni} = U_{Mn} = 3$ eV were chosen for further electronic structure, electric polarization, and spin flop transition calculations unless mentioned otherwise.

The orbital-resolved partial density of states (PDOS) of YNMO in the FM order is shown in Fig. S2(c). The electronic structures of d states for $Ni^{2+}(d^8)$ and $Mn^{4+}(d^3)$ are displayed in Fig. S2(d). The five spin-up electrons of Ni^{2+} occupy the t_{2g} and e_g orbitals, and three spin-down electrons occupy the t_{2g} orbital. For the Mn^{4+} ions, three spin-up electrons fill half the t_{2g} orbital. The five d states of Ni^{2+} reduce degeneracy due to Jahn–Teller distortion, so that the energy level of Ni^{2+} d_{xy} is higher than d_{yz}/d_{xz}. The occupied t_{2g} states of Mn^{4+} and the unoccupied e_g orbital of Ni^{2+} should contribute to the Ni-O-Mn super-exchange interaction and has a further impact on the exchange interactions.

The geometrically optimized structure in the ↑↑↓↓-type order indicates the direction of off-centering displacements [Fig. 2(a)] of Ni, Mn, and O ions, which corresponds to the initial $P2_1/n$ symmetry. Indeed, the off-centering relative displacements lead to an alternate long–short–long–short interlayer distance, with $d^{p} = 3.70$ Å and $d^{ap} = 3.72$ Å, whereas d_{center} is 3.708 A in the experimental FM central symmetry structure.[17] In addition to the displacements along the c-axis, the main displacement vectors are along the -b axis. In the Y_2NiMnO_6 system, the ↑↑↓↓-type order makes the O sites to become nonequivalent, i.e., one between spin-ordered Ni and Mn ions with parallel spins (labeled as O_p) and the others between spin-ordered Ni and Mn ions with anti-parallel spins (labeled as O_{ap}). Besides the spin order on the Ni and Mn ion sites, the nonequivalent sites of oxygen atoms are also spin-polarized (the induced magnetic moments of O_p and O_{ap} are 0.02 u_B, 0.03 u_B, respectively). The nonequivalent of was further demonstrated by the spin density plot in Fig. 2(b). Therefore, the spin order of the ↑↑↓↓-type state leads to the contribution of electrons to the whole electron polarization. By using the Berry-phase calculation (supplementary material), the electronic contribution to the total electric polarization is also along the -b axis. Different from the cases in $HoMnO_3$,[4] the direction of $\vec{P}_{ion}$ is opposite to that of $\vec{P}_{ele}$, but the two contributions have the same order of magnitude and does not have full offset for $\vec{P}_{ele}$. For the ↑↑↓↓-type phase in Y_2NiMnO_6, the calculations show the total electric polarization of 0.78 $\mu C/cm^2$ along the b-axis and agree well with the experimental reports, which found that the polarization of single crystals is also along the b-axis.

The spin flop transition will take place when a strong magnetic field is applied along the easy axis of sublattice magnetization. In YNMO, when a large enough magnetic field is applied along the easy axis, the ↑↑↓↓-type order will transform into FM order. In order to explore the mechanism of magnetoelectric coupling and spin flop transition in YNMO, we calculated the energy and polarization dependence on the orientation of spin flop. As shown in Fig. 3, according to the expression of Zeeman magnetic field energy, it is assumed that the total energy E is due to the sum of the Zeeman energies of the individual sublattices and a term representing the exchange coupling, which will depend on the relative orientation between the two sublattice moments. This leads to

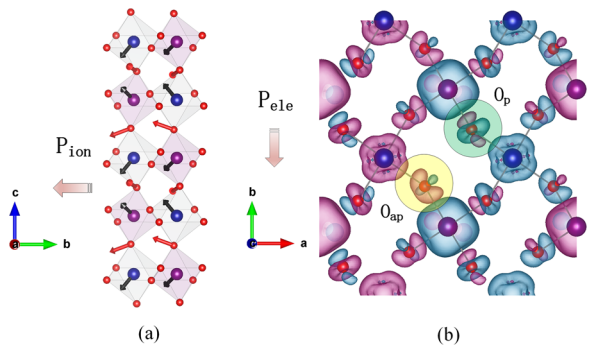

FIG. 2. (a) Calculated directions of ion displacements of Ni, Mn, and O ion. The black and red arrows denote the directions of the displacement of Ni/Mn and O ions. (b) The *ab*-plane spin density isosurface plot for ↑↑↓↓-type order. Red gradient arrows denote the direction of electric polarization.

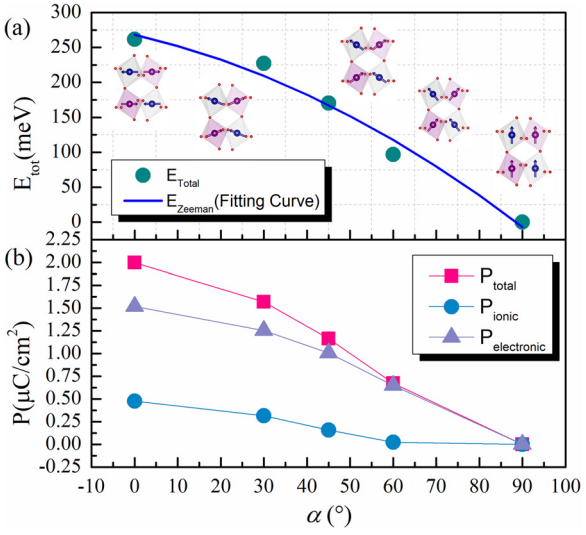

FIG. 3. (a) Energy of the E-type order dependence on the direction of rotation spin in the *ac*-plane of YNMO; the blue line is the fitting curve according to the Zeeman expression of magnetic field energy. (b) Electric polarization dependence on the spin flop angle.

$$E = -MB\cos\alpha - MB\cos\beta + AM^2\cos(\alpha+\beta) - \frac{1}{2}\Delta\left(\cos^2\alpha + \cos^2\beta\right), \quad (7)$$

where A is a constant connected with the exchange coupling, M is the magnetization, and B is the magnetic field strength. To ignore the magnetic anisotropy Δ and make the spin flop angle $\alpha = \beta$, we could have

$$E = -2MB\cos\alpha + AM^2\cos 2\alpha. \quad (8)$$

To satisfy the E-type order, we build a $2 \times 1 \times 1$ supercell, constrain the spin along the *a*-axis as the initial state, and then rotate the spin orientation along the *ac*-plane, and the final state is the FM order along the *c*-axis (see Fig. S3). We can see from Fig. 3(a) that the total energies decrease as the angle increases. The curve is obtained by quadratic fitting; the corresponding coefficient is $MB = 1.41$ eV and $A = -0.018$ eV. These results can explain the mechanism of strong magnetic field-induced spin flop. One can see from Fig. 3(b) that the electric polarization also decreased as the spin flop angle increased. As we discussed above, the E-type order corresponds to the ↑↑↓↓-type order along the (101) plane. In addition to the magnetic-striction mechanism, a compatible contribution from the redistribution of polarized charge is found in the present study. The crystal structure change with the spin flop angle is listed in Table II.

The ↑↑↓↓-type order displays two scenarios E_1 and E_2 for the domain boundaries [as shown in the insets of Fig. 4(a)]. The two diverse kinds of AFM domains were predicted to show opposite electric polarizations $\vec{P}_{tot}$ and $-\vec{P}_{tot}$. Therefore, we design a FE-AFM switching path from $P_{\uparrow\uparrow\downarrow\downarrow}$ (E_1) to $P_{\uparrow\downarrow\downarrow\uparrow}$ (E_2) through a progressive rotation of the even-layer spin directions from 0° to 180° and fix the odd-layer spins. Indeed, turning even-layer spin from 0° to 180°, there is an energy change with structural distortion, which increases from E_1 to $E_\perp$ and decreases from $E_\perp$ to E_2. As shown in Fig. 4(b), the total electric polarization decreases from $\vec{P}_{\uparrow\uparrow\downarrow\downarrow}$ to $\vec{P}_\perp$ and increases from $\vec{P}_\perp$ to $\vec{P}_{\uparrow\downarrow\downarrow\uparrow}$ in the opposite direction. We, thus, describe the following important conclusion for YNMO: ↑↑↓↓-type order induces symmetry breaking from the center symmetry group $P2_1/n$ to a polar group $P2_1$, which turns the system into a stable ferroelectric phase. Furthermore, the spin rotation not only leads to the distortions in ionic off-centering displacements but also induces the charge redistribution, and the variations in interlayer distances are calculated along the polar axis (Fig. S5). The exchange striction mechanism is further confirmed by spin rotation. Indeed, we also design an adiabatic path by gradually rotating the Ni/Mn spins in even-layers from 0° to 180° along the *ac*-plane and from the paraelectric to ferroelectric state (Fig. S4).

In summary, we have systematically investigated the intrinsic role of ↑↑↓↓-type order in magnetoelectric coupling in Y_2NiMnO_6.

TABLE II. The calculated lattice constants and Ni–O–Mn bond angle dependence on the spin flop angle.

Spin flop angle	a(Å)	b(Å)	c(Å)	θ (°)
0°	10.3641	5.5358	7.4148	144.14
30°	10.3632	5.5337	7.4176	144.48
45°	10.3647	5.5311	7.4209	144.67
60°	10.3653	5.5282	7.4244	145.01
90°	10.3679	5.5209	7.4319	145.27

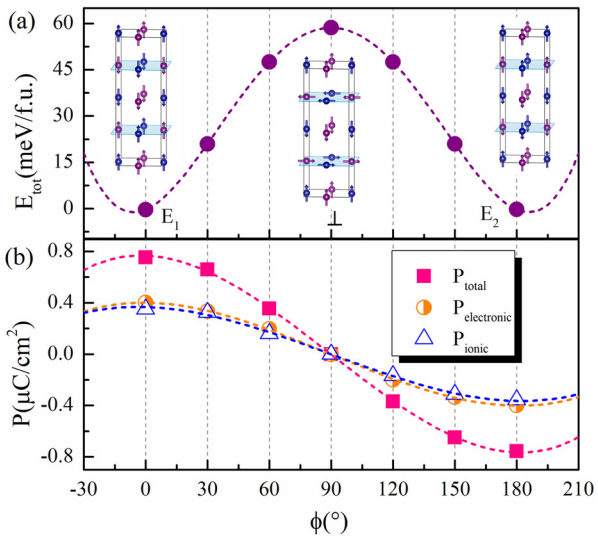

FIG. 4. (a) Total energy vs the orientation of the even-layer spins (blue marked regions in the plot in the inset denote the layers of spin rotation). (b) Total electric polarization calculated via berry phase methods' dependence on the orientation of the even-layer spin.

The calculated results reveal that the FM order is the magnetic structure of the ground state. Our DFT+U results indicate that the total energy of ↑↑↓↓-type order is close to that of the FM order. The electric polarization is calculated to be 0.78 μC/cm^2 along the crystallographic *b*-axis for $U_{Ni} = U_{Mn} = 3$ eV. In addition to the exchange-striction mechanism, a more noticeable contribution from redistribution of polarized charge is found in our study. Magnetic hysteresis loops show the ferromagnetism in YNMO, which can be explained by magnetic field-induced spin flop transition from the E-type to FM order. Our DFT+U theoretical investigations also proposed a switching adiabatic path of magnetoelectric coupling, in which the 180° reverse of electric polarization is driven by rotation of spins.

See the supplementary material for the magnetic structure of Y_2NiMnO_6; calculated Ni–O–Mn super-exchange angles, exchange interaction coefficients, and PDOS; Berry-Phase methods; schematic illustration of the direction of spin flop transition in the E-type magnetic structure; and schematic illustration of the direction of spin rotation.

This work was supported financially by the Development Program for Outstanding Young Teachers in the Chang Chun University of Science and Technology (CUST) (Grant No. XQNJJ-2018–06) and the Science and Technology Research project of the Jilin Provincial Department of Education (Grant No. JJKH20200732KJ). We thank the High Performance Computing Center of the School of Advanced Materials, Peking University, Shenzhen Graduate School for calculation resources.

DATA AVAILABILITY

The data that support the findings of this study are available within this article and its supplementary material.

REFERENCES

[1]D. V. Efremov, J. Van der Brink, and D. I. Khomskii, Nat. Mater. **3**, 853 (2004).
[2]N. A. Spaldin and M. Fiebig, Science **309**, 391 (2005).
[3]W. Eerenstein, N. D. Mathur, and J. F. Scott, Nature **442**, 759 (2006).
[4]S. Picozzi, I. A. Sergienko, K. Yamauchi, B. Sanyal, and E. Dagotto, Phys. Rev. Lett. **99**, 227201 (2007).
[5]S. Lee, A. Pirogov, M. Kang, K. H. Jang, M. Yonemura, T. Kamiyama, S. W. Cheong, F. Gozzo, N. Shin, H. Kimura, Y. Noda, and J. G. Park, Nature **451**, 805–808 (2008).
[6]M. Mostovoy, Phys. Rev. Lett. **96**, 067601 (2006).
[7]J. van der Brink and D. I. Khomskii, J. Phys.: Condens. Matter. **20**, 434217 (2008).
[8]G. Sharma, J. Saha, S. D. Kaushik, V. Siruguri, and S. Patnaik, Appl. Phys. Lett. **103**, 012903 (2013).
[9]S. K. Upadhyay, P. L. Paulose, and E. V. Sampathkumaran, Phys. Rev. B **96**, 014418 (2017).
[10]L. Zhao, H. Guo, W. Schmidt, K. Nemkovski, M. Mostovoy, and A. C. Komarek, Phys. Rev. B **96**, 54424 (2017).
[11]H. Katsura, N. Nagaosa, and A. V. Balatsky, Phys. Rev. Lett. **95**, 057205 (2005).
[12]Y. Tokura, S. Seki, and N. Nagaosa, Rep. Prog. Phys. **77**, 076501 (2014).
[13]A. Narayan, A. Cano, A. V. Balatsky, and N. A. Spaldin, Nat. Mater. **18**, 223 (2019).
[14]L. Xu, J. Meng, Q. Liu, J. Meng, X. Liu, and H. Zhang, Phys. Chem. Chem. Phys. **22**, 4905 (2020).
[15]H. Wu, T. Burnus, Z. Hu, C. Martin, A. Maignan, J. C. Cezar, A. Tanaka, N. B. Brookes, D. I. Khomskii, and L. H. Tjeng, Phys. Rev. Lett. **102**, 026404 (2009).
[16]S. Kumar, G. Giovannetti, J. van den Brink, and S. Picozzi, Phys. Rev. B **82**, 134429 (2010).
[17]H. Nhalil, H. S. Nair, C. M. N. Kumar, A. M. Strydom, and S. Elizabeth, Phys. Rev. B **92**, 214426 (2015).
[18]J. Su, Z. Yang, X. Lu, J. Zhang, L. Gu, C. Lu, Q. Li, J. Liu, and J. Zhu, ACS Appl. Mater. Interfaces **7**, 13260 (2015).
[19]H. T. Chen, Y. Ni, and A. K. Soh, J. Appl. Phys. **113**, 134102 (2013).
[20]H. Y. Zhou, H. J. Zhao, W. Q. Zhang, and X. M. Chen, Appl. Phys. Lett. **106**, 152901 (2015).
[21]G. Kress and J. Furthmüller, Phys. Rev. B **54**, 11169 (1996).
[22]G. Kress and D. Joubert, Phys. Rev. B **59**, 1758 (1999).
[23]P. E. Blöchl, Phys. Rev. B **50**, 17953 (1994).
[24]S. L. Dudarev, G. A. Botton, Y. Y. Savrasov, C. J. Humphreys, and A. P. Sutton, Phys. Rev. B **57**, 1505 (1998).
[25]W. Kohn and L. J. Sham, Phys. Rev. **140**, A1133 (1965).
[26]H. J. Monkhorst and J. D. Pack, Phys. Rev. B **13**, 5188 (1976).
[27]R. D. King-Smith and D. Vanderbilt, Phys. Rev. B **47**, 1651 (1993).
[28]K. Momma and F. Izumi, J. Appl. Crystallogr. **44**, 1272–1276 (2011).
[29]A. Kaippamagalath, J. P. Palakkal, A. P. Paulose, and M. R. Varma, Ferroelectrics **518**, 223–231 (2017).
[30]E. O. Wollan and W. C. Koehler, Phys. Rev. **100**, 545–563 (1955).